

Article ID: 1006-8775(2016) 01-0057-09

FUTURE CHANGE OF PRECIPITATION EXTREMES OVER THE PEARL RIVER BASIN FROM REGIONAL CLIMATE MODELS

DU Yao-dong (杜尧东)^{1,2}, YANG Hong-long (杨红龙)², CAO Chao-xiong (曹超雄)³, LIU Wei-qin (刘蔚琴)¹
(1. Climatic Center of Guangdong Province, Guangzhou 510080 China; 2. Shenzhen National Climate Observatory, Shenzhen 518040 China; 3. Guangzhou Institute of Tropical and Marine Meteorology/Guangdong Provincial Key Laboratory of Numerical Modeling, China Meteorological Administration, Guangzhou 510080 China)

Abstract: Based on RegCM4, a climate model system, we simulated the distribution of the present climate (1961-1990) and the future climate (2010-2099), under emission scenarios of RCPs over the whole Pearl River Basin. From the climate parameters, a set of mean precipitation, wet day frequency, and mean wet day intensity and several precipitation percentiles are used to assess the expected changes in daily precipitation characteristics for the 21st century. Meanwhile the return values of precipitation intensity with an average return of 5, 10, 20, and 50 years are also used to assess the expected changes in precipitation extremes events in this study. The structure of the change across the precipitation distribution is very coherent between RCP4.5 and RCP8.5. The annual, spring and winter average precipitation decreases while the summer and autumn average precipitation increases. The basic diagnostics of precipitation show that the frequency of precipitation is projected to decrease but the intensity is projected to increase. The wet day percentiles (q90 and q95) also increase, indicating that precipitation extremes intensity will increase in the future. Meanwhile, the 5-year return value tends to increase by 30%-45% in the basins of Liujiang River, Red Water River, Guihe River and Pearl River Delta region, where the 5-year return value of future climate corresponds to the 8- to 10-year return value of the present climate, and the 50-year return value corresponds to the 100-year return value of the present climate over the Pearl River Delta region in the 2080s under RCP8.5, which indicates that the warming environment will give rise to changes in the intensity and frequency of extreme precipitation events.

Key words: climate change; RCPs scenario; Pearl River Basin; regional climate model; RegCM4

CLC number: P426.61.4 **Document code:** A

doi: 10.16555/j.1006-8775.2016.01.007

1 INTRODUCTION

Extreme climate events, such as floods, droughts, rainstorms, high temperature, etc, have been frequently on the rise, resulting in significant increases in direct economic loss and posing wide serious impacts on societal, economic and ecological environment of the mankind, and drawing widespread attention from all walks of life. As shown in increasing amount of evi-

dence, the increase of the concentration of green-house gases may increase the regional extreme precipitation events (EPEs) (Wehner^[1]), even in areas where mean precipitation is falling (Groisman and Karl^[2]). There have been some work on climate change for different main river basins in China in recent years (Jiang et al.^[3]; Zeng et al.^[4]; Liu et al.^[5]; Kang et al.^[6]; Xu et al.^[7]; Shi et al.^[8]). Located in the monsoon region of the South China Sea (SCS) that is sensitive to climate change (Du et al.^[9]), the Pearl River Basin (PRB) is composed of complicated types of underlying surface and subject to frequent occurrence of EPEs. Heavily populated and economically developed (Feng and Yang^[10]), PRB suffers much more seriously in economy due to natural disasters resulting from climate change. It is therefore of important significance for assessing the effect of climate change, making adaptive counter-measures, improving the capabilities of disasters mitigation and adapting to climate change to investigate into the variation of EPEs in the PRB under the background of global climate. At present, research on the climate change of the PRB focuses on the spatio-temporal evolution of the mean state of historical precipitation (Liu et al.^[11]; Liu et al.^[12]) and characteristics of historical precipitation extremes (Lu et al.^[13]; Peng et al.^[14]), while study on estimating future climate change is all based on the output under the e-

Received 2014-12-22; **Revised** 2015-10-19; **Accepted** 2016-01-15

Foundation item: Specialized Research Project for Public Welfare Industries (Meteorology) from the Ministry of Science and Technology (GYHY201406025); Specialized Project for Climate Change from China Meteorological Administration (CCSF201404, CCSF2011-25, CCSF201211CCSF 2011-25); Specialized Foundation for Low Carbon Development in Guangdong Province (2012-019); Foundation of Science Innovation Teams for Guangdong Meteorological Bureau (201102); Science and Technology Planning Project for Guangdong Province (2012A061400012)

Biography: YANG Hong-long, Ph.D., Senior Engineer, primarily undertaking research on regional climate change and environmental meteorology.

Corresponding author: YANG Hong-long, e-mail: yangh01@163.com

mission scenario of Intergovernmental Panel on Climate Change Special Report on Emissions Scenarios (IPCC SRES) (Huang et al.^[15, 16]; Liu et al.^[17, 18]). In its fifth assessment report, IPCC projected a set of scenarios of representative concentration pathways, or RCPs (Moss et al.^[19]; Wang et al.^[20]), in which the scenarios targeted the concentration rather than radiative forcing and have been used by modeling teams of different countries in computation of climate change and effect assessment. Using the output of global models, Xu et al.^[21, 22] analyzed the future variations of temperature and precipitation averaged over China under the emission scenario of RCPs.

With the data of emission scenarios of the PRB under RCP4.5 and RCP8.5 provided by National Climate Center of China, this work characterized the variation of precipitation extremes in the basin for a past period of 1980-1999 and a future one of 2010-2099 against a series of precipitation indexes. Estimating and analyzing in detail the frequency and intensity of precipitation as well as the EPEs, this study aims to providing reliable information for estimation of future climate in the PRB, complete and scientific fundamental research achievements for assessment of climate change effect and formulation of adaptive counter-measures, and references for making the third national assessment report on climate change in China.

2 MODEL, DATA AND METHODOLOGY

2.1 Model and data

The data of emission scenarios under the RCPs are provided by the National Climate Center of China(Ji^[23]). One-way nested between a global climate model

(BCC_CSM1.1) and a regional climate model (RegCM4), the modeling domain covers the whole region of China but only the PRB is chosen for this study (Fig.1). Developed by the Abdus Salam International Center for Theoretical Physics of Italy, the RegCM is one of the representative regional climate models that have been used and applied extensively. The RegCM4 is the latest version of RegCM. Using the dynamic framework of MM5, the model employs the σ -coordinates in the vertical and the alternative mesh of Arakawa B in the horizontal. Having a horizontal resolution of $0.5^\circ \times 0.5^\circ$, it is divided into 18 layers in the vertical with the top layer at 100 hPa. For detailed parameters, refer to Pal et al.^[24].

Driven by BCC_CSM1.1, a global climate model, for the boundary field and initial field, the RegCM4 obtains the data of daily precipitation under the two emission scenarios of RCP8.5 and RCP4.5, referred to as BCC85 and BCC45 respectively hereafter. The data spans from 1980 to 1999 and from 2010 to 2099. Taking the period of 1980-1999 as reference, the time from 2010 to 2039 is set as the 2020s, that from 2040 to 2069 the 2050s, and that from 2070 to 2099 the 2080s. The atmospheric model of BCC_CSM1.1 is BCC-AGCM2.1, with resolution at T_{42} and gridpoints at intervals of 2.8° . Its modules of land surface, ocean and sea ice are BCC-AVIM, MOM4 and SIS respectively. The data used in the model include the aerosols of sulphate, sea salt, black carbon, organic carbon and dust and at intervals of 10a. Only the direct effect of aerosols is considered in the model. In addition, the model also uses the monthly data of volcano-erupted aerosol by Ammann et al.^[25]. Besides, this paper also us-

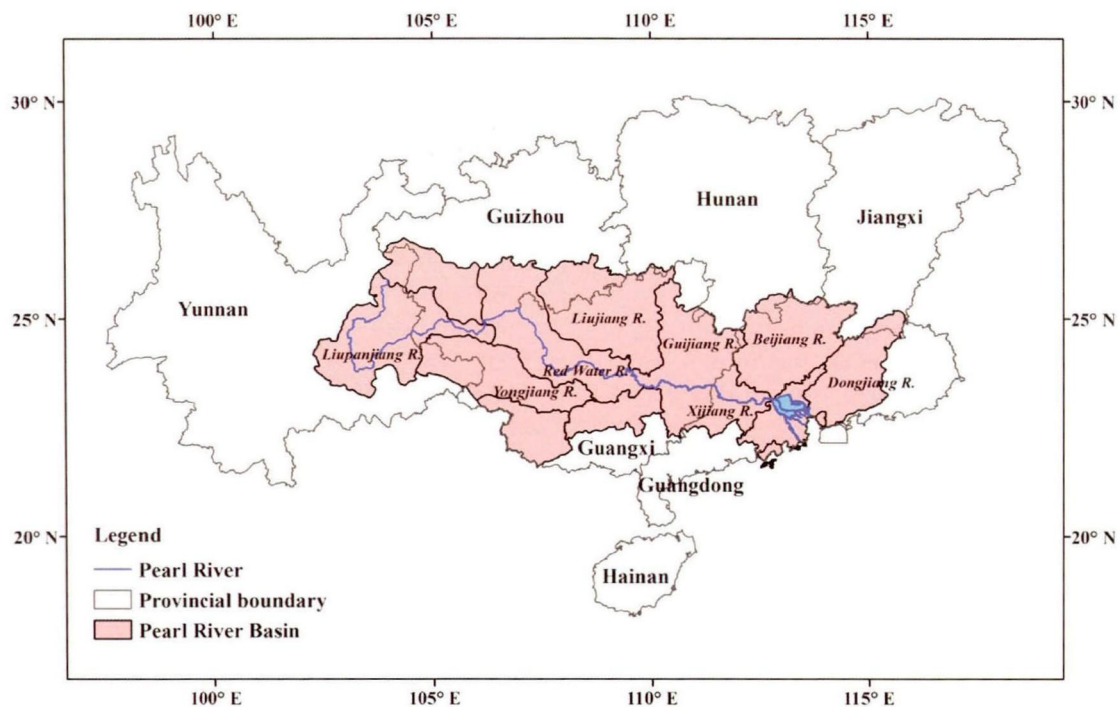


Figure 1. Geographic distribution of the PRB.

es a series of high-resolution ($0.5^\circ \times 0.5^\circ$) meshed data, gathered from over 700 sites of observation, referred to as XIE hereafter, of daily mean precipitation developed in recent years by Xie et al.^[26]. In the emission scenario of RCP8.5, three main types of green-house gases, i.e. CO₂, CH₄ and N₂O, are described in terms of the time-dependent variation of emission, concentration and radiative forcing, with the last item higher than the emission scenario of A2, the high level of emission with the SRES, and that of A1F1 with the concentrated type of fossil fuel. In the emission scenario of RCP4.5, however, these green-house gases are predicted to peak in 2040, with their concentration and radiative forcing tending to stabilize in 2070 following a medium, stable pathway.

2.2 Indexes and methods

To study the variations of precipitation comprehensively, this paper uses a series of diagnostic indexes (as shown in Table 1) to characterize the distribution of rainfall intensity from moderate to extreme levels. The daily mean precipitation, wet day frequency and mean wet day intensity are used as basic items to diagnose the occurrence and intensity of precipitation. Used to describe the coverage of precipitation, percentiles reflect the distribution of rainfall intensity but are independent of the wet day frequency. For depicting the characteristics of precipitation extremes, the values of maximum daily rainfall intensity in returns of 5, 10, 20, 50 and 100 years are used. In this paper, the computation of return values follows the widely-used Gumbel fitting distribution. In China, the Gumbel fitting distribution was used to study the return periods of precipitation extremes in various parts of the country (Xie et al.^[27]; Wei et al.^[28]), e.g. the northwest part of China (Wei et al.^[28]), to analyze the variation trends of precipitation extremes. Additionally, to verify how well the theoretic distribution of extreme events fits the observed distribution and taking into account the purpose of current study being on the fitting distribution of small-sized samples, the Kolmogorov test is used here to verify the fitting results. The method works by testing the deviation of the empirical distribution function, determined with samples, from an assumed theoretic distribution function.

Table 1. Indicators of precipitation.

Indicator	Definition	Unit
mea	Daily mean rainfall	mm/d
fre	Wet day frequency, wet day if daily rainfall>1mm	times
int(SDII)	Simplified daily rainfall intensity, wet day mean rainfall	mm/d
qXX ^a	Percentile of rainfall (XX%) during wet days	mm/d
X1d.TT ^b	Return values of 1-day precipitation intensity with a return period of TT	mm/d

Note: XX^a=90% or 95%; TT^b=5, 10, 20, 50, 100 years.

2.2.1 GUMBEL DISTRIBUTION

The Gumbel distribution is a typical theoretic model that describes the statistical distribution of extremes. Its distribution function can be expressed as:

$$F(x)=P(X_{\max}<x)=\exp(-\exp(-\alpha(x-u))) \quad \alpha>0, -\infty < u < \infty \quad (1)$$

where $\alpha>0$ is the scale parameter and u the position parameter. For fitting the distribution of extremes, the typical Gumbel approach is used to estimate the distribution parameter.

2.2.2 KOLMOGOROV TEST

First, assume that the overall distribution function $F(x)$ is consistent with the theoretic distribution function $G_0(x)$, or, $F(x)=G_0(x)$, then $d_n = \left| F_n^*(x_m^*) - G_0(x_m^*) \right|$, the deviation on each of the points, can be derived. Then, determine d_n , the maximum deviation. If n is very large, then $d_n \sqrt{n}$ approximately follows the distribution of $\theta_n(\lambda)$. And then, locate the critical value of λ_α that meets $\theta(\lambda_\alpha) = 1 - \alpha$ based on the degree of confidence α . λ_α can be known by looking up in the table of Kolmogorov functions. In the final step, compare $d_n \sqrt{n}$ with λ_α . If $d_n \sqrt{n} < \lambda_\alpha$, accept the original assumption. Reject it if otherwise is true.

3 RESULTS AND ANALYSIS

3.1 Verification of model

Table 2 gives the distribution of observed and simulated mean precipitation on the yearly and seasonal ba-

Table 2. Statistical distribution of the observed and simulated characteristics of precipitation of the PRB for the reference period (1980-1999).

Time		Obs.	Sim.	Sim./Obs.
Year	mea/(mm/d)	4.2	4.3	1.0
	fre/times	128.3	202.9	1.6
	int/(mm/d)	10.7	7.6	0.7
	q90	26.5	16.8	0.6
	q95	37.6	26.8	0.7
Spring	mea/(mm/d)	4.5	5.3	1.2
	fre/ times	35.0	57.9	1.7
	int/(mm/d)	10.7	8.3	0.8
	q90	26.2	18.6	0.7
	q95	36.7	28.5	0.8
Summer	mea/(mm/d)	7.6	7.1	0.9
	fre/ times	50.2	74.2	1.5
	int/(mm/d)	12.6	8.7	0.7
	q90	31.3	19.5	0.6
	q95	44.2	33.2	0.8
Autumn	mea/(mm/d)	3.0	2.5	0.8
	fre/ times	25.9	32.4	1.2
	int/(mm/d)	9.5	6.6	0.7
	q90	25.0	16.8	0.7
	q95	36.6	29.2	0.8
Winter	mea/(mm/d)	1.5	2.5	1.7
	fre/ times	17.1	38.5	2.2
	int/(mm/d)	6.3	5.5	0.9
	q90	15.4	12.3	0.8
	q95	21.4	18.2	0.8

sis in the PRB over the reference period, which shows that in the model simulation the annual mean precipitation is consistent with the observation while the precipitation frequency (fre) is higher but the rainfall intensity (int) and wet day percentiles (q90 and q95) are lower than the observation. In the PRB, precipitation is the most in summer, followed by spring and autumn, and the least in winter. The model is successful in simulating the trend of precipitation in the four seasons, though with small amount for summer and autumn and large amount for spring and winter. For the four seasons, the simulation is relatively small in precipitation frequency but relatively large in precipitation intensity, especially in winter (with a ratio of 2.2). For the wet day percentiles of the four-season precipitation, the simulation is about 20% smaller.

Figure 2 gives the distribution of the observed and simulated 5-year return values of 1-day precipitation extremes in the PRB. During the time, the X1d.5 varies from 80 to 160 mm/d, which shows a decreasing gradient from the southeast (coast) to the northwest (inland) (see Fig.2a). The model simulations show consistent trends of variation with the observation. For the Liupan-

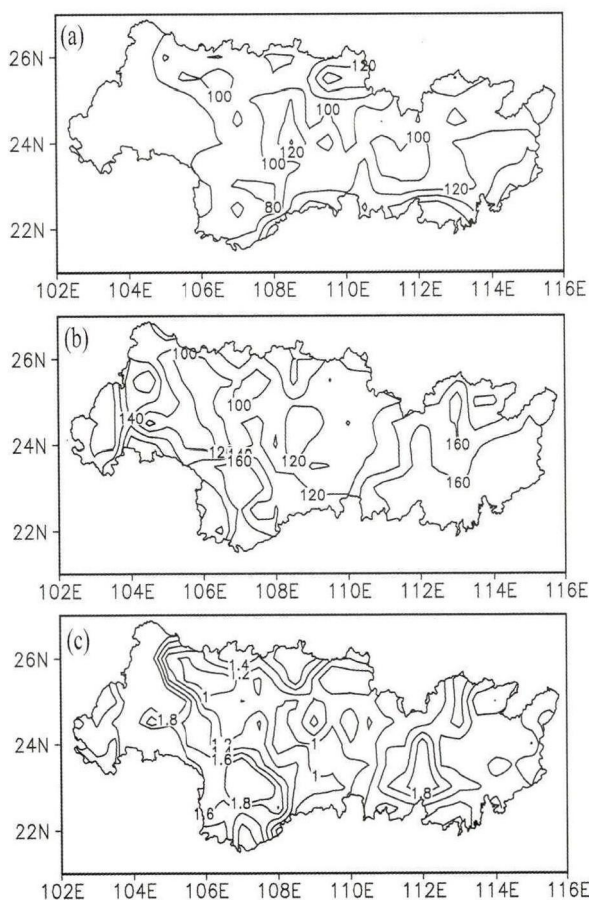


Figure 2. Spatial distribution of the observed and simulated 5-year return values of 1-day precipitation extremes over the reference period in the PRB. a: observations; b: simulations; c: ratios of simulations to observations.

jiang River (LPJ R.) and Yijiang River (YJ R.) basins in the northwestern part of the PRB, the observed daily precipitation is from 80 to 100 mm/d, or with the ratio of simulation to observation ranging from 1.4 to 2.0. For the basins of Red Water R., Liujiang River (LJ R.), Guijiang River (GJ R.) and Xijiang River (XJ R.) in the middle of the PRB, the simulation is close to the observation while it is about 40% to 60% larger than the observation in Dongjiang River (DJ R.), Beijiang River (BJ R.) and Pearl River Delta (PRD) in the eastern part of the PRB (see Fig.2c). Generally speaking, the model does a good job in simulating the large-scale spatial distribution of X1d.5 in the PRB though with larger simulations in some parts.

3.2 Variations of the basic characteristics of precipitation in the future periods

Figure 3 gives the distribution of precipitation characteristics averaged over the year and four seasons in the future periods in the PRB under the emission scenario of RCP4.5. Compared to the simulated values in the reference period, all characteristic values of precipitation but mean rainfall amount differ significantly in the future. In the future, the annual mean rainfall will decrease in the PRB, with its ratio to that of the reference period varying from 0.98 to 1.0 in the future periods of 2020s, 2050s and 2080s. Showing different trends of variation, seasonal average rainfall will decrease by about 3% in spring, a larger reduction than that of the annual mean. It will increase in summer and autumn, with the latter season having the largest increment, winter having the largest reduction, and the mean reduction being about 10% for all future periods. Such decreasing trends are also found in the annual mean precipitation frequency, about 4% for different periods. Except in the summers of the 2050s and 2080s when the reduction is generally unchanged (within 1%), the precipitation frequency all shows decreasing trends ranging from 2% to 16% in all other seasons of the remaining periods. It is especially noted that the reduction is as much as 16% in the winter of the 2080s. The reduction of annual mean rainfall amount and precipitation frequency result in the increase of rainfall intensity and by 2% to 4% as far as the intensity of the annual mean rainfall is concerned. With the exception of spring, the rainfall intensity for all the other three seasons tend to be increasing, with the amplitude being the largest in autumn, followed by winter and then by summer, the least.

When the total amount of precipitation remains unchanged or increases while the frequency decreases, it may indicate the presence of a possible intensifying trend with the rainfall process (Zhai and Ren^[29]). In the future periods, the trends of the simulations are consistent with those of the observation and the annual mean values of q90 and q95 are increasing, and so are their increments over time. Except for the wet day percentiles of spring precipitation, the values of all the other sea-

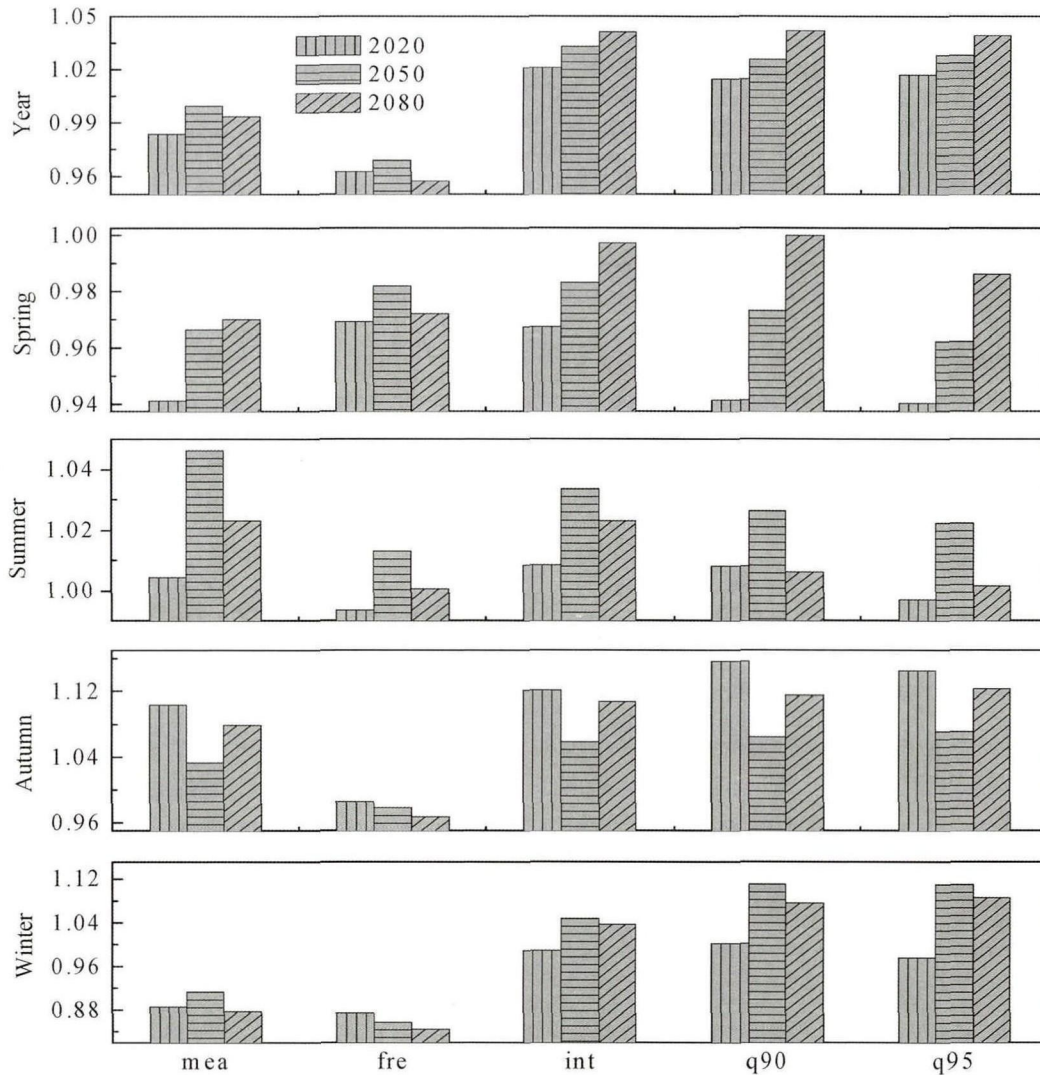


Figure 3. Simulated change (ration future/ reference) in mean precipitation diagnostics under the emission scenario of RCP4.5.

sions are increasing, with the amplitude being the largest in autumn and the smallest in summer. In the autumn of all future periods, the increments of q90 ad q95 are between 5% and 14% in autumn while being about 4% in the summer of all the other future periods.

Under the emission scenario of RCP8.5 (figure omitted), the variations of precipitation averaged over the year and four seasons in the PRB over the future periods are similar to those of RCP4.5 scenario, with decreased overall rainfall amount and frequency but increased rainfall intensity, thus leading to the increase of quantile of precipitation (q90 and q95). Precipitation varies differently in the four seasons, with increased amount in summer and autumn but decreased amount in winter and spring. The precipitation frequency decreases but the intensity increases in the four seasons, resulting in the increase of quantile of precipitation (q90 and q95) for all seasons.

It is known from the annual variations of precipitation characteristics in the future periods under the two

emission scenarios (Fig.4) that they have generally similar trends with the scenarios of RCP8.5 and RCP4.5 though the annual variations and amplitude changes are much more significant with the former scenario. Over time, these trends will become more obvious. In other words, the trends of precipitation variation with the higher-emission scenario (RCP8.5) will be getting more obvious to result in greater probabilities for EPEs.

Figure 5 gives the variations of 5-year return values of 1-day precipitation extremes in the periods of 2050s and 2080s relative to those of the reference period. In the period of 2020s (Fig.5), the X1d.5 will increase by a range from 0% to 5% in most of the PRB region, with the basins of LJ R., Red Water R., GJ R. and PRD area having the largest amplitude of increase (more than 30%) and some parts of the basins of LJ R. and Red Water R. and Pearl R. having as much as 45% increase. In contrast, X1d.5 is decreasing in LPJ R., southern YJ R., eastern XJ R. and DJ R. by amplitudes less than 20%. For the period of 2050s (Fig.5), the val-

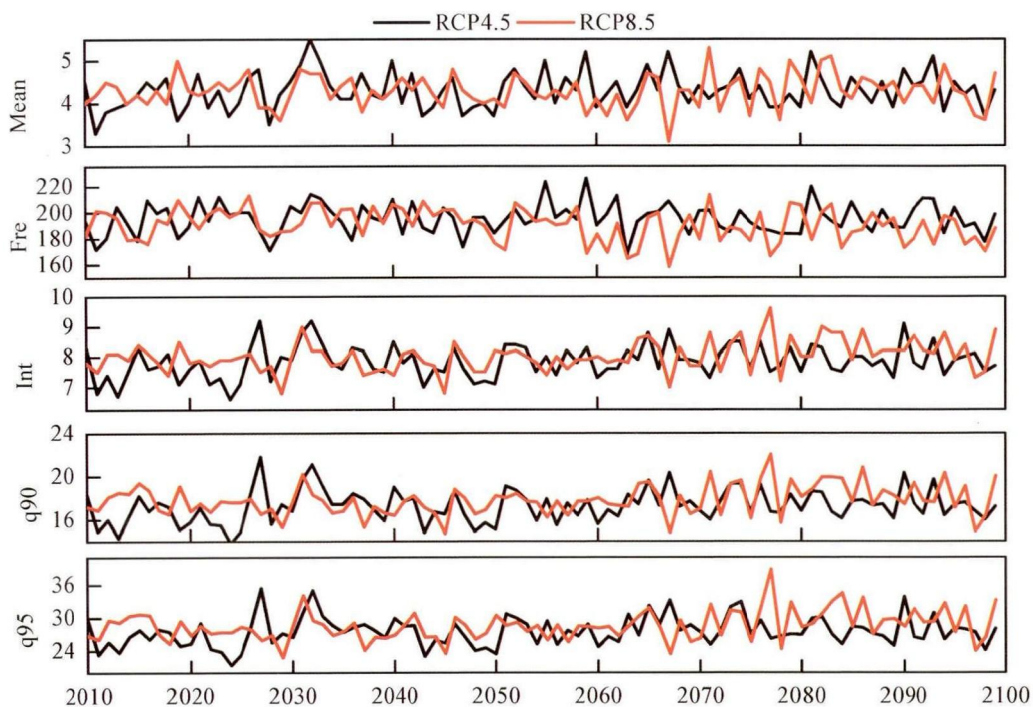


Figure 4. Comparisons of the temporal variations of annual mean precipitation characteristics in the PRB under RCP4.5 and RCP8.5. The abscissa is for the year.

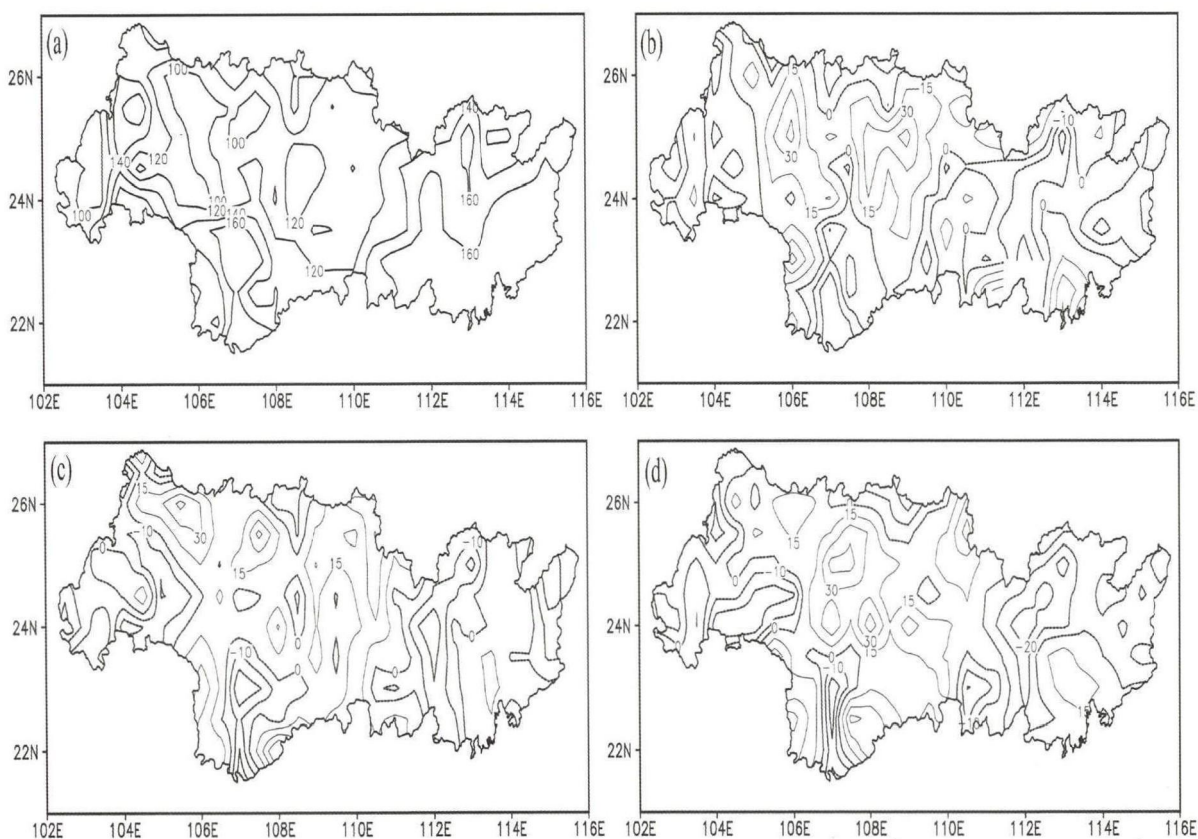


Figure 5. Variations of 5-year return values of 1-day precipitation intensity for different future periods in the PRB relative to the reference period under the emission scenario of RCP4.5. Units: %: (a): reference period; (b): 2020s; (c): 2050s; (d): 2080s.

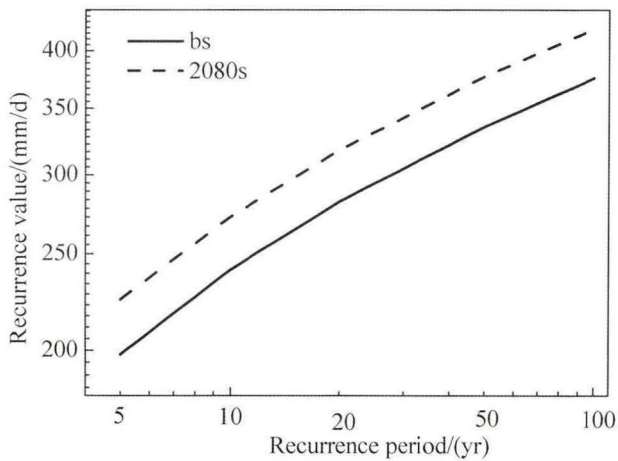


Figure 6. Annual return values of 1-day precipitation intensity for the 2080s period and the reference period in the PRD under the emission scenario of RCP8.5.

ue of X1d.5 varies in much the same way as that of the reference period and the areas of reduction are basically the same. The large-value area moves to the east and shifts to the basins of LJ R., Red Water R. and GJ R., with the maximum increment more than 45%. For the period of 2080s (Fig.5d), the value of X1d.5 decreases in areas consistent with that of the 2050s period and the large-value area moves towards the west relative to that of the 2020s period, located in the area bordering the LJ R. basin and Red Water R. basin. The amplitude of increase is more than 45%.

Under RCP8.5, the value of X1d.5 increases by 15% to 45% in the 2020s, 2050s and 2080s periods in most of the PRB region (figure omitted). For the 2020s period, the increment is more than 15% in most of the PRB region, with GJ R., Red Water R. and the area joining XJ R. and YJ R. having the largest increment (more than 45%). For the 2050s period, the basins of Red Water R., XJ R. and YJ R. also have increments that are larger than 45%. For the 2080s period, the increment is within 15% in most of the PRB region while the southern YJ R. basin, southwestern XJ R. basin, northern BJ R. and PRD area have amplitudes that are larger than 30%.

Through analyzing X1d.5, it is known that precipitation extremes change in different parts of the PRB in the future periods under different scenarios. To study in greater detail the trends of variation of the precipitation extremes, this work compares the mean values of the annual maximum daily rainfall between the reference period and the 2080s period under the RCP8.5 in the PRD area (Fig.6). The model-simulated values of the 5-year return in future periods are equivalent of those in 8 to 10 years of the current period, the future 20-year return values are equivalent of those in 40 to 50 years of the current period, and the future 50-year return values are equivalent of those in 100 years of the current period.

4 CONCLUDING REMARKS

Using BCC_CSM1.0, a one-way nested global climate model in the regional climate model of RegCM4, this work characterizes the variations of precipitation in the PRB over the reference period (1980–1999) and the future period (2010–2099) under the latest emission scenarios of RCP4.5 and RCP8.5. Mean rainfall, wet days and simple daily rainfall intensity are used to diagnose basically the frequency and intensity of precipitation. Independent of precipitation frequency, the value of precipitation percentile is used to describe the spatial extent of precipitation and reflect the distribution of precipitation intensity. The characteristics of precipitation extremes are depicted with the values of annual maximum daily precipitation intensity in the return periods of 5, 10, 20, 50 and 100 years.

(1) Under the emission scenarios of RCP4.5 and RCP8.5, mean precipitation and precipitation frequency will decrease but precipitation intensity will increase in the PRB in the future periods. For all future periods, mean precipitation will decrease in spring and winter but increase in summer and autumn; the precipitation intensity will decrease in spring but increase in the other three seasons. Such changes in the basic characteristics of precipitation result in the increase of the wet day percentiles (q90 and q95) in all future periods; they decrease in spring but increase in the other three seasons. The largest increment happens in autumn, followed by winter, with summer having the least increment.

(2) A growing trend is found in the EPEs (indicated by X1d.TT) of the PRB in the future periods. They increase by 30% to 45% in the basins of LJ R., Red Water R., GJ R. and the PRD area but decrease by about 20% in the basins of LP R., southern YJ R., eastern DJ R. and DJ R. Under the emission scenario of RCP8.5, the mean values of the 5-year return in future periods are equivalent of those in 8 to 10 years of the current period, the future 20-year return values are equivalent of those in 40 to 50 years of the current period, and the future 50-year return values are equivalent of those in 100 years of the current period.

This work attempts to study the climate change on regional scale using a high-resolution regional model. The simulated precipitation is still with large uncertainties and the simulations need to be improved in the future. In spite of it, differences do remain in different models with the change of emission scenarios (Huang et al.^[16]; Liu et al.^[18]). Changes in the precipitation characteristics include decreased precipitation frequency and increased precipitation intensity and the wet day percentiles, reflecting the trends of basic features of precipitation in the future periods under different emission scenarios in different models (Yang^[30]; Song^[31]). The increase of precipitation extremes is much larger than that of mean precipitation, possibly because the change in mean precipitation is controlled by the equilibrium of

energy while the change in precipitation extremes is related to the condensation of efficient water vapor in the atmospheric column and its intensity increases with the growth of efficient water content. The increase in the wet day percentiles may be subject to the restriction of the Clapeyron-Clausius relation (Boer^[32]).

Acknowledgement: The authors would like to express their gratitude towards GAO Xue-jie and XU Ying, research fellows from the National Climate Center of China for their provision of the data of climate scenarios and network observations. It is also appreciated that Professor CAO Chao-xiong has voluntarily translated the whole paper into English.

REFERENCES:

- [1] WEHNER M. Predicted twenty-first-century changes in seasonal extreme precipitation events in the parallel climate model [J]. *J Climate*, 2004, 17(21): 4 281-4 290.
- [2] GROISMAN P Y, KARL T R, EASTERLING D. Changes in the probability of heavy precipitation: Important indicators of climatic change [J]. *Climate Change*, 1999, 42(1): 243-283.
- [3] JIANG Tong, SUN Bu-da, WANG Yan-jun. Trends of Temperature, Precipitation and Runoff in the Yangtze River Basin from 1961 to 2000. *Advances in climate change research* [J]. 2005, 1(2): 65-68.
- [4] ZENG Xiao-fan, SU Bu-da, JIANG Tong, et al. Projection of future climate change in the Yangtze River Basin for 2001-2050 [J]. *Adv Climate Change Res*, 2007, 3 (5): 293-298.
- [5] LIU Lv-liu, LIU Zhao-fei, XU Zong-xue. Trends of climate change for the upper-middle reaches of the Yellow River in the 21st Century [J]. *Adv Climate Change Res*, 2008, 4 (3): 167-172.
- [6] KANG Li-li, WANG Shou-rong, GU Jun-qiang. The simulation test of the distributed hydrological model DHSVM on the runoff change of Lanjiang River basin [J] *J Trop Meteorol*, 2008, 24(2): 176-181.
- [7] XU Y, XU C, GAO X, et al. Projected changes in temperature and precipitation extremes over the Yangtze River Basin of China in the 21st century [J]. *Quatern Int*, 2009, 208 (1): 44-52.
- [8] SHI Y, GAO X, ZHANG D, et al. Climate change over the Yarlung Zangbo -Brahmaputra River Basin in the 21st century as simulated by a high resolution regional climate model [J]. *Quatern Int*, 2011, 244: 159-168.
- [9] DU Yao-dong, SONG Li-li, MAO Hui-qing, et al. Climate warming in Guangdong province and its influences on agriculture and the adaptation measures [J]. *J Trop Meteorol*, 2004, 20(3): 302-310.
- [10] FENG Yan, YANG Xiao-ling. Preliminary study on the general plan for the ecological construction project in the Zhujiang River valley [J]. *Forest Res Manage*, 2004, 20 (3): 302-310.
- [11] LIU Bing-jun, CHEN Xiao-hong, ZENG Zhao-fa. Spatial distribution law of rainfall in the lower reaches of the pearl river basin [J]. *J Nat Res*, 2010, 25 (12): 2 123-2 131.
- [12] LIU Yan-qun, CHEN Chuang-mai, ZHENG Yong. The characteristics of spatial distribution and types of Apr-Sept rainfall in the river basin [J]. *J Trop Meteorol*, 2008, 24(1): 67-73.
- [13] LU Hong, CHEN Si-rong, GUO Yuan, et al. Spatial-temporal variation characteristics of extremely heavy precipitation frequency over south China in the last years [J]. *J Trop Meteorol*, 2012, 28(2): 219-227.
- [14] PENG Jun-tai, ZHANG Qiang, CHEN Xiao-hong, et al. Spatial and temporal evolution characteristics of extreme rainfalls in the Pearl River Basin [J]. *J Catastroph*, 2011, 26(4): 24-28.
- [15] HUANG Xiao-yin, TAN Hao-bo, LI Fei, et al. Changes of flood-season severe precipitation over South China in the 21st century [J]. *Meteorol Sci Technol*, 2009, 37(4): 425-428.
- [16] HUANG Xiao-yin, WEN Zhi-ping, DU Yao-dong, et al. Scenario analyses on the changes of future surface air temperature and precipitation south China [J]. *J Trop Meteorol*, 2008, 24(3): 254-258.
- [17] LIU Lv-liu, JIANG Tong, XU Jin-ge, et al. Responses of hydrological processes to the climate change in the Zhujiang River Basin in the 21st Century [J]. *Adv Climate Change Research*, 2012, 8(1): 28-34.
- [18] LIU Lv-liu, DAN Tong, YUAN Feng. Observed (1961-2007) and projected (2011-2060) climate change in the Pearl River Basin [J]. *Adv Climate Change Res*, 2009, 5(4): 209-214.
- [19] MOSS R, EDMONDS J, HIBBARD K, A E. The next generation of scenarios for climate change research and assessment [J]. *Nature*, 2009, 463(7282): 747-756.
- [20] WANG Shao-wu, ZHAO Jun-ci, LUO Yong, et al. Observed (1961-2007) and projected (2011-2060) climate change in the Pearl River Basin [J]. *Adv Climate Change Res*, 2012, 8(4): 305-307.
- [21] XU H C, XU Y. The projection of temperature and precipitation over China under RCP scenarios using a CMIP5 multi-model ensemble [J]. *Atmos Ocean Sci Lett*, 2012, 5(6): 527-533.
- [22] XU H C, XU Y. Preliminary assessment of simulations of climate changes over China by CMIP5 multi-models [J]. *Atmos Ocean Sci Lett*, 2012, 5(6): 489-494.
- [23] JI Zheng-ming. *Climate change in China as simulated by a high resolution regional climate model under new emission scenarios* [R]. Institute of Tibetan Plateau Research, Chinese Academy of Sciences, 2012
- [24] PAL J S, GIORGI F, BI X. The ICTP RegCM3 and RegCNET: Regional climate modeling for the developing world [J]. *Bull Amer Meteorol Soc*, 2007, 9(88): 1 395-1 409.
- [25] AMMANN C M, MEEHL G A, WASHINGTON W M, et al., A monthly and latitudinally varying volcanic forcing dataset in simulations of 20th century climate [J]. *Geophys Res Lett*, 2003, 30(12): 87-104.
- [26] XIE P, YATAGAI A, CHEN M, et al. A gauge-based analysis of daily precipitation over East Asia [J]. *J Hydrometeorol*, 2007, 8(3): 607-626.
- [27] XIE Zhi-qing, JIANG Ai-jun, DING Yu-guo. Spatial-temporal features of annual extremes of heavy precipitation processes in the Yangtze River Delta [J]. *J Nanjing Inst Meteorol*, 2005, 28(2): 267-274.
- [28] WEI Feng, DING Yu-guo, BAI Hu-zhi. Simulation tests of temporal spatial distributions of precipitation extremes over China based on probability weighted moments estimation [J]. *Adv Earth Sci*, 2005, 20: 65-70.

- [29] ZHAI Pan-mao, REN Fu-ming. Detection of trends in China's precipitation extremes [J]. J Meteorol Res, 1999, 2(57): 208-216.
- [30] YANG Hong-long. Scenario analyses on future change of extreme climate events over China using PRECIS [D]: Lanzhou university, 2010
- [31] SONG Rui-yan. Projected future changes of extreme precipitation climate events over china by a high resolution regional climate model (RegCM3) [D]: Chinese academy of meteorological sciences, 2008
- [32] BOER G. Climate change and the regulation of the surface moisture and energy budgets [J]. Clim Dyn, 1993, 8 (5): 225-239.

Citation: DU Yao-dong, YANG Hong-long, CAO Chao-xiong, et al. Future change of precipitation extremes over the Pearl River basin from regional climate models [J]. J Trop Meteorol, 2016, 22(1): 57-65.